Human Cancer Biology

Clinical Cancer Research

Validation of SAG/RBX2/ROC2 E3 Ubiquitin Ligase as an Anticancer and Radiosensitizing Target

Lijun Jia, Jie Yang, Xinbao Hao, Min Zheng, Hongbin He, Xiufang Xiong, Liang Xu, and Yi Sun

Abstract

Purpose: Sensitive to apoptosis gene (SAG; also known as RBX2 or ROC2) was originally cloned as a redox-inducible antioxidant protein and was later characterized as a RING component of SCF E3 ubiquitin ligases. SAG overexpression inhibits apoptosis induced by many stimuli both *in vitro* and *in vivo*. SAG mRNA was overexpressed in human lung tumor tissues with a correlation to poor patient survival. To investigate whether SAG serves as an anticancer target, we determined the effect of SAG silencing on cell proliferation, survival, and radiosensitivity.

Experimental Design: SAG protein expression in human tumors was evaluated by immunohistochemical staining using tumor tissue arrays. SAG expression in cancer cells was knocked down by siRNA silencing. The anticancer effects of SAG silencing were evaluated by *in vitro* assays for cell growth and survival and by an *in vivo* orthotopic xenograft tumor model. Radiosensitization by SAG silencing of human cancer cells was determined by clonogenic survival assay. Apoptosis induction was evaluated by fluorescence-activated cell sorting analysis, caspase-3 activation assay, and Western blotting of apoptosis-associated proteins.

Results: SAG was overexpressed in multiple human tumor tissues compared with their normal counterparts. SAG silencing selectively inhibited cancer cell proliferation, suppressed *in vivo* tumor growth, and sensitized radiation-resistant cancer cells to radiation. Mechanistically, SAG silencing induced apoptosis with accumulation of NOXA, whereas SAG overexpression reduced NOXA levels and shortened NOXA protein half-life.

Conclusions: The findings showed that SAG E3 ubiquitin ligase plays an essential role in cancer cell proliferation and tumor growth and may serve as a promising anticancer and radiosensitizing target.
Clin Cancer Res; 16(3); 814–24.

The ubiquitin-proteasome system controls protein turnover and regulates a variety of signaling pathways and cellular processes, from cell proliferation to differentiation to death (1). Recent studies showed that pharmacologic inhibition of the ubiquitin-proteasome system can be efficacious in the treatment of human cancers. Bortezomib (Velcade, formerly PS-341) represents the first Food and Drug Administration–approved proteasome inhibitor to treat multiple myeloma and hematologic as well as solid tumors (2). It mainly blocks the activation of NF-κB and induces the proapoptotic protein NOXA, rendering cells apoptotic (2, 3). The fast-track approval of bortezomib has spurred a great wave of interest in the development of anticancer reagents against the ubiquitin-proteasome system.

The Skp1-Cullin1-F-box-protein (SCF) E3 ubiquitin ligases are multiunit complexes and consist of scaffold proteins (cullin 1-cullin 7), RING-finger proteins (RBX1/ROC1 or RBX2/SAG), adaptor proteins (e.g., Skp1), and F-box proteins (e.g., Skp2 and Fbw7; refs. 4, 5). They mediate the transfer of ubiquitin molecules to substrates (substrate polyubiquitination) for subsequent recognition and degradation by proteasome. Because SCF E3 ubiquitin ligases control the degradation of a variety of protein substrates through the ubiquitin-proteasome system to regulate diverse cellular processes, SCF dysfunction could cause a variety of diseases, including cancer. For example, oncogenic F-box proteins Skp2 and β-TrCP, which promote the degradation of tumor suppressor p27 or IκB, respectively, were overexpressed in several human cancers, which is associated with a higher degree of malignancy and poor patient prognosis (6). On the other hand, mutation or deletion of tumor suppressor F-box protein Fbw7 caused the accumulation of several oncogenic protein substrates, such as c-Jun, c-Myc, cyclin E, and mammalian target of rapamycin, leading to accelerated tumor cell proliferation and tumorigenesis (7, 8). Most recently, we found that the

Authors' Affiliation: Division of Radiation and Cancer Biology, Department of Radiation Oncology, University of Michigan Comprehensive Cancer Center, Ann Arbor, Michigan

Note: Supplementary data for this article are available at Clinical Cancer Research Online (http://clincancerres.aacrjournals.org/).

Corresponding Author: Yi Sun, University of Michigan, 4424B Medical Science Building, 1301 Catherine Street, Ann Arbor, MI 48109-5637. Phone: 734-615-1989; Fax: 734-763-1581; E-mail: sunyi@umich.edu.

doi: 10.1158/1078-0432.CCR-09-1592

Translational Relevance

The interest in the development of anticancer drugs against the ubiquitin-proteasome system has been spurred by the fast-track Food and Drug Administration approval of the proteasome inhibitor bortezomib (also known as Velcade or PS-341) for the treatment of relapsed and refractory multiple myeloma. Skp1-Cullin1-F-box-protein complexes, the largest multiunit E3 ubiquitin ligases, target a variety of substrates for degradation through the ubiquitin-proteasome system and regulate carcinogenesis and cancer progression. We show here that sensitive to apoptosis gene (SAG), the second member of the RBX/ROC RING component of Skp1-Cullin1-F-box-protein E3 ubiquitin ligases, is a promising anticancer target with the following observations: (*a*) SAG is overexpressed in several human primary cancers, particularly lung cancer; (*b*) SAG siRNA silencing selectively kills cancer *in vitro* and *in vivo*; and (*c*) SAG siRNA silencing selectively sensitizes radioresistant cancer cells to radiation. Thus, the development of small molecules or RNA interference–based therapy targeting SAG holds a promise for future treatment of human cancer.

RING-finger protein RBX1/ROC1 was overexpressed in diverse human primary tumors, and downregulation of RBX1 by RNA interference silencing inhibited cancer cell growth through activation of multiple cell killing pathways, including cell cycle arrest, apoptosis, and senescence (9). These findings suggested that the SCF E3 ubiquitin ligase complexes could function as anticancer targets.

Sensitive to apoptosis gene (SAG) was originally cloned in our laboratory as a redox-inducible antioxidant protein and was later characterized as the second member of the RBX/ROC RING component of SCF E3 ubiquitin ligases (10–12). As an antioxidant, SAG overexpression inhibits apoptosis induced by redox (10, 13), nitric oxide (14), ischemia/hypoxia (15), heat shock (16), neurotoxin, and 1-methyl-4-phenylpyridinium (17) *in vitro* and *in vivo*. When complexed with other components of SCF E3 ubiquitin ligase, SAG has E3 ubiquitin ligase activity and promotes the stage-dependent degradation of c-Jun and IκBα, thus regulating carcinogenesis and tumor growth in a 7,12-dimethylbenz(*a*)anthracene–12-*O*-tetradecanoylphorbol-13-acetate murine skin cancer model (18). In human lung cancers, SAG mRNA was significantly overexpressed in tumor tissues with a correlation to poor patient survival (19). The findings suggest that SAG E3 ubiquitin ligase may be required for human carcinogenesis or progression and serve as an anticancer target.

Here, we showed that SAG protein was overexpressed in multiple human primary tumor tissues, particularly in lung cancer. SAG siRNA silencing had no effect on normal cell growth, but inhibited the growth of cancer cells, both *in vitro* and *in vivo* by induction of apoptosis. Moreover, SAG silencing sensitized radioresistant H1299 and U87 cells to ionizing radiation. Thus, SAG may serve as a target for anticancer therapy as well as radiosensitization.

Materials and Methods

Cell culture. H1299 human lung cancer cells, U87 human glioblastoma cells, PANC-1 human pancreatic carcinoma cells, and MRC-5 lung fibroblast cells were purchased from the American Type Culture Collection and cultured in DMEM with 10% fetal bovine serum (FBS). Normal bronchial epithelial cells, NL20, were grown in Ham's F-12 medium with 4% FBS and essential supplements, as previously described (20).

Immunohistochemical staining of human tumor tissue arrays. Multiple human tumor tissue arrays were provided and stained with purified SAG monoclonal antibody (mAb) by the University of Michigan Comprehensive Cancer Tissue Core. Briefly, 5-μm tissue array sections were dehydrated and subject to peroxidase blocking. SAG mAb [raised against the RING domain (AA44-113)] was added at a dilution of 1:100 and incubated at room temperature for 30 min on the DAKO AutoStainer using the DakoCytomation EnVision+ System-HRP (DAB) detection kit. The slides were counterstained with hematoxylin (Surgipath). The stained slides were observed under a microscope (Olympus 1X71) and images were acquired using software DP controller (ver. 3.1.1.267, Olympus).

Lentivirus-based siRNA and lentivirus infection. Construction and preparation of lentivirus-based siRNA against SAG (LT-SAG) and lentivirus expressing scrambled control siRNA (LT-CONT) were previously described (21). The target sequences are as follows: LT-SAG02-01, 5′-AACAAGAGGACTGTGTTGTGGTCTGGTTCAAGAGACCAGACCACAACACAGTCCTCTTGTTTTTTGT-3′; LT-SAG02-02, 5′-CTAGACAAAAAACAAGAGGACTGTGTTGTGGTCTGGTCTCTTGAACCAGACCACAACACAGTCCTCTTGTT-3′; LT-CONT-01, 5′-ATTGTATGCGATCGCAGACTTTTCAAGAGAAAGTCTGCGATCGCATACAATTTTTTGT-3′; and LT-CONT-02, 5′-CTAGACAAAAAATTGTATGCGATCGCAGACTTTCTCTTGAAAAGTCTGCGATCGCATACAAT-3′.

ATPlite cell proliferation assay. Cells were infected with LT-SAG or LT-CONT for 96 h, then split and seeded into 96-well plates with 3,000 cells per well in quadruplicate. At 24, 48, 72, and 96 h after cell plating, cell proliferation assay using the ATPlite 1 step luminescence ATP detection assay system (Perkin-Elmer) was done according to the manufacturer's instruction (22).

Clonogenic survival assay. Cells were infected with LT-SAG or LT-CONT for 96 h, then split and seeded into six-well plates at 100 cells (H1299 and Panc-1) or 300 cells (U87) per well in triplicate, followed by incubation at 37°C for 9 d. The colonies formed were fixed with 10% acidic acid in methanol, stained with 0.05% methylene blue, and counted.

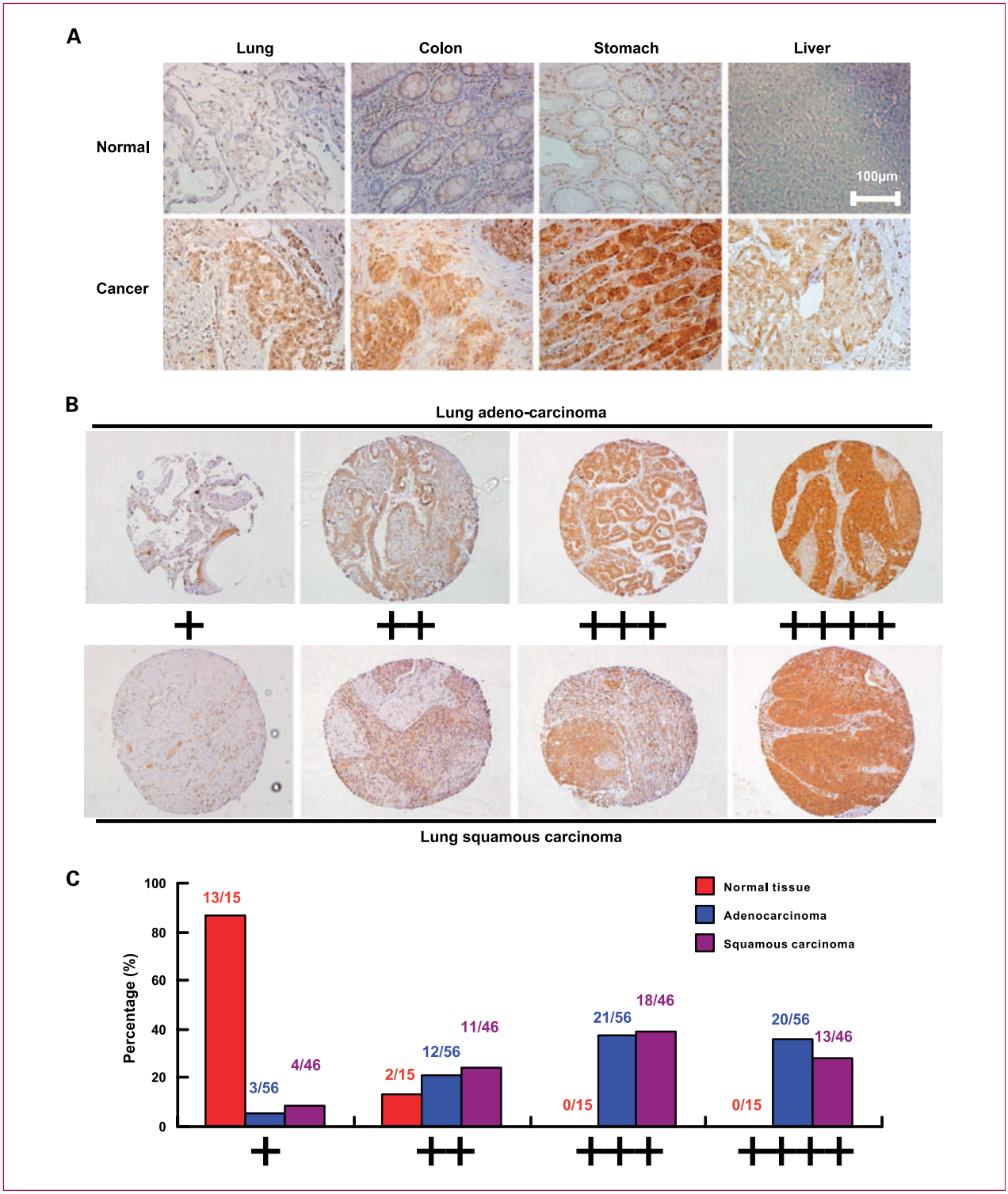

Fig. 1. The expression of SAG in human tumors and normal counterparts. A, SAG overexpression in multiple human primary tumor tissues. Tumor tissue arrays containing multiple normal and tumor tissues from different organs were stained with purified SAG mAb on the DAKO AutoStainer using the DakoCytomation EnVision+ System-HRP (DAB) detection kit and counterstained with hematoxylin (Surgipath). The stained slides were observed under a microscope (Olympus 1X71) and images were acquired using software DP controller. B, SAG staining in lung tissues, normal versus cancer. Lung tumor tissue arrays containing normal lung and tumor tissues were stained for SAG expression. Stained normal and tumor tissues were classified into four groups (+ to ++++) according to the staining intensity of each tissue. C, percentage of normal or tumor tissues in each staining group. Tissue samples with different staining intensity were grouped and tabulated.

Soft agar assay. Ten thousand cells after lentivirus-based siRNA silencing were seeded in 0.33% agar containing 1× cell culture medium and 10% FBS in 60-mm Petri dish and grown at 37°C for 14 d. The cells were stained with *p*-iodonitrotetrazolium (1 mg/mL; Sigma) overnight and the colonies were counted (21).

Irradiation and radiosensitization assay. Cells, after lentivirus-based siRNA silencing, were seeded in six-well plates at three different cell densities in duplicate. The next day, cells were exposed to different doses of radiation followed by incubation at 37°C for 9 d. The colonies formed were fixed, and the surviving fraction was determined by the proportion of seeded cells following irradiation that formed colonies relative to untreated cells, as previously described (20).

Fluorescence-activated cell sorting analysis. H1299 and U87 cells were infected with LT-SAG, along with LT-CONT, for 96 h, then split and cultured for 72 h, followed by propidium iodide staining and fluorescence-activated cell sorting (FACS) analysis for apoptosis detection. Briefly, infected cells were harvested and fixed in 70% ethanol at −20°C for 4 h, stained with propidium iodide (18 μg/mL) containing 400 μg/mL RNase A (Roche), incubated with shaking for 1 h, and analyzed by flow cytometry for apoptosis and cell cycle profile, as previously described (22). Apoptosis was measured by the percentage of cells in the sub-G_1 population.

Western blotting analysis. Whole-cell lysates were prepared and subjected to immunoblotting analysis using antibodies against SAG [mAb raised against the RING domain (AA44-113)], Bax, Bad, cIAP2 (Cell Signaling), pRB, Puma, Mcl-1 (Santa Cruz Biotechnology), XIAP, Bcl-XL, p21 (BD Transduction Laboratories), β-actin (Sigma), Bak (Upstate), Bim (Imgenex), NOXA (Oncogene Science), Bcl-2 (DAKO), and survivin (Novus Biologicals).

Orthotopic pancreatic tumor model. Panc-1 cells stably transfected with luciferase reporter were infected with LT-CONT or LT-SAG for 96 h and were used to establish an orthotopic model of pancreatic tumor, as previously described (23). Briefly, cells (2×10^6 per mouse in a volume of 0.1 mL) were injected orthotopically into the pancreata of nude mice as follows. Five mice in each group were anesthetized; a small left abdominal flank incision was made; and tumor cells were injected into the subcapsular region of the pancreas using a 30-gauge needle and a calibrated push button–controlled dispensing device. A cotton swab was held cautiously for 1 min over the site of injection to prevent leakage. The peritoneum and skin incision were closed sequentially with absorbable suture. After 5 weeks, tumors were bioluminescence imaged using a cryogenically cooled imaging system coupled to a data acquisition computer running Living Image software at the University of Michigan magnetic resonance imaging core. Mice were then sacrificed and tumors were harvested and weighed.

Caspase-3 activation assay. Cells were infected with LT-SAG, along with LT-CONT, for 96 h, then split and seeded in 96-well plates at 1.5×10^4 per well for incubation at 37°C for 72 h. The cells were then lysed and subjected to a fluorogenic caspase-3 assay with Ac-DEVD-AFC as substrate (Biomol; ref. 22). The results were expressed as fold change compared with control. Each treatment had three replicates.

Half-life analysis of NOXA. To evaluate the effect of SAG overexpression on the half-life of NOXA, U87 cells cultured in six-well cell culture plates were transiently transfected with FLAG-NOXA in combination with FLAG-SAG or pcDNA3 with a total of 2 μg DNA per well (1 μg FLAG-NOXA plus 1 μg FLAG-SAG or pcDNA3) for 24 h. The transfected cells were then treated with 20 μg/mL cycloheximide. Protein samples were collected at 0, 1, 2, 4, and 8 h after cycloheximide treatment and subjected to NOXA detection using anti-FLAG antibody by Western blotting analysis with β-actin as the loading control.

To determine the effect of SAG knockdown on the half-life of endogenous NOXA, U87 cells were infected with LT-SAG, along with LT-CONT, for 96 h and then split and seeded into six-well cell culture plates. Twenty-four hours later, cells were treated with 20 μg/mL cycloheximide for the indicated periods of time, followed by Western blotting using antibody against endogenous NOXA, with β-actin as the loading control. The relative Noxa levels were quantified by densitometry analysis using the ImageJ1.410 image processing software.

Statistical analysis. The statistical significance of differences between groups was assessed using the GraphPad Prism4 software (version 4.03). The unpaired two-tailed *t* test was used for the comparison of parameters between groups. The level of significance was set at $P < 0.05$.

Results

SAG is overexpressed in human primary tumor tissues. Overexpressed SAG was previously shown in human lung cancer tissues by reverse transcription-PCR (19) and in a subset of colon cancer by Western blotting (24). These studies might underestimate SAG overexpression in cancer tissues due to normal tissue contamination and tumor stromal cell infiltration. To precisely determine the expression status of SAG in human tumor tissues, we performed immunostaining analysis using a SAG mAb raised against purified human SAG RING domain (AA44-113) fused with glutathione *S*-transferase (Creative Biolabs). The antibody specificity against SAG was validated by immunofluorescent staining to detect SAG in wild-type mouse embryonic stem cells, but not in SAG knockout embryonic stem cells.[1] This specific mAb was then used to measure the SAG levels in human cancer tissue microarrays. As shown in Fig. 1A, SAG was expressed weakly in several normal tissues (*top*) but was overexpressed in a panel of human tumor tissues, including carcinomas of the lung, colon, stomach, and liver

[1] Unpublished data.

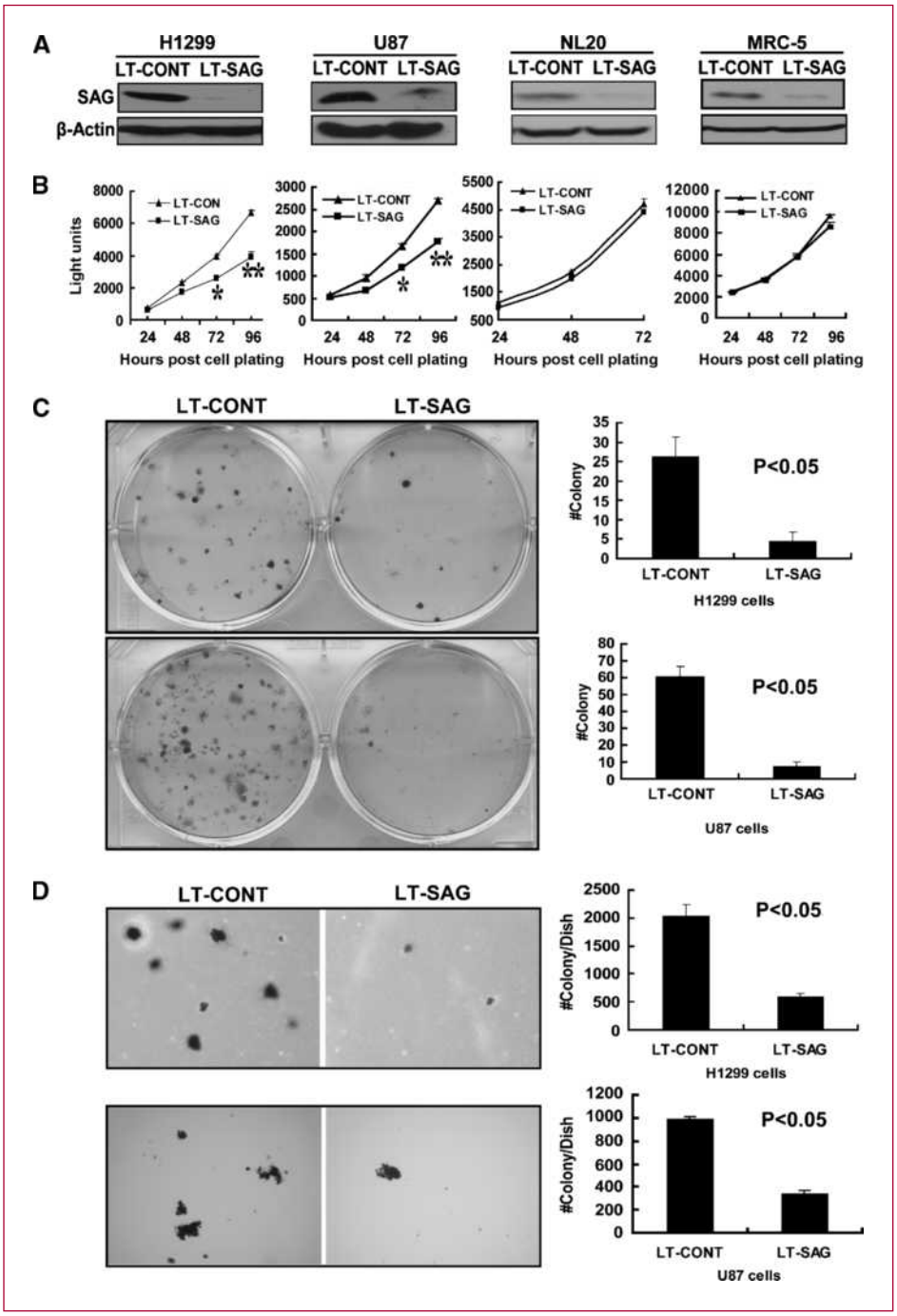

Fig. 2. SAG silencing selectively inhibits the growth of human cancer cells. H1299 human lung cancer cells, U87 human glioblastoma cells, NL20 normal bronchial epithelial cells, and MRC-5 lung fibroblast cells were infected with LT-CONT and LT-SAG for 96 h and then split for assays as follows. A, SAG silencing effects were determined by immunoblotting, with β-actin as the loading control, 96 h after cell splitting. B, ATPlite cell proliferation assay. Cells, after lentivirus-based siRNA silencing, were split and seeded into 96-well plates at 3,000 per well in quadruplicates and subjected to ATPlite cell proliferation assay over periods up to 96 h. *, $P < 0.05$; **, $P < 0.01$. C, clonogenic cell survival assay in H1299 (top) and U87 (bottom) cells. Cells, after lentivirus-based siRNA silencing, were split, seeded into six-well plates at 100 cells (H1299) or 300 cells (U87) per well in triplicates, and incubated at 37°C for 9 d, followed by 0.05% methylene blue staining and colony counting. D, soft agar anchorage-independent growth assay in H1299 and U87 cells. Ten thousand cells after lentivirus-based siRNA silencing were seeded in 0.33% agar containing 1× cell culture medium and 10% FBS in 60-mm Petri dish, then grown at 37°C for 14 d, followed by staining with *p*-iodonitrotetrazolium overnight and colony counting.

(*bottom*). To focus on lung cancer, we immunostained two sets of human lung cancer tissue arrays, consisting of 15 normal tissues and 102 tumor tissues of adenocarcinoma ($n = 56$) and squamous carcinoma ($n = 46$). Based on the intensity of staining, we classified the samples into four groups, with group 1 showing the least staining (+) and group 4 the highest staining (++++; Fig. 1B). We found that the SAG staining in normal tissues was under either group 1 (13 of 15, 87%) or group 2 (2 of 15, 13%), whereas most tumor tissues, regardless of tumor types, had a high SAG staining (mainly in cancer cells, but not in stromal cells) and were classified into groups 3 and 4 (73% for adenocarcinoma and 67% for squamous carcinoma; Fig. 1C). Thus, SAG is overexpressed in most human lung cancers. The overexpression of SAG in diverse primary human tumors suggests that SAG could play a role in carcinogenesis or in the maintenance of tumor cell phenotype.

SAG silencing inhibits the growth of human cancer cells. We next determined, using siRNA knockdown approach, the role of SAG in the regulation of cell proliferation of tumor versus normal cells by an ATPlite assay. As shown in Fig. 2A, SAG silencing by LT-SAG (21) caused a reduction in SAG expression of more than 90% in H1299 non–small cell lung carcinoma cells (*blot 1*), in U87 glioblastoma cells (*blot 2*), in NL20 normal bronchial epithelial cells (*blot 3*), and in MRC-5 lung fibroblast cells (*blot 4*). Consequently, cell proliferation was inhibited significantly in H1299 and U87 cells (Fig. 2B, graphs 1 and 2). Interestingly, the normal cells were rather resistant to SAG knockdown with very minor growth inhibition (Fig. 2B, graphs 3 and 4), indicating a tumor cell–selective growth suppression. We next determined the effect of SAG silencing on tumor cell survival by clonogenic assay. As shown in Fig. 2C, SAG silencing caused an 80% or 85% inhibition in survival of H1299 or U87 cells, respectively. Furthermore, the anchorage-independent growth of H1299 and U87 cells, as measured by soft agar assay, was inhibited by up to 75% on SAG silencing (Fig. 2D). These findings indicate that SAG silencing significantly suppresses the growth and survival of human cancer cells, but is rather inactive during normal cell growth.

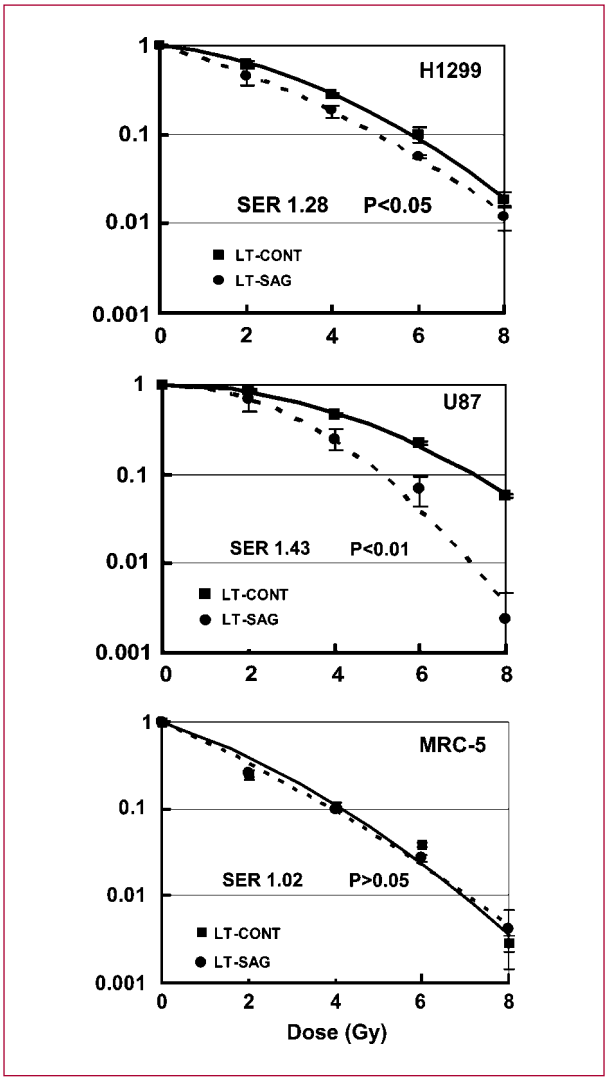

Fig. 3. SAG silencing sensitizes cancer cells to radiation. Cells, after lentivirus-based siRNA silencing, were seeded in six-well plates at three different cell densities in duplicates. The next day, cells were exposed to different doses of radiation followed by incubation at 37°C for 9 d for colony counting. The surviving fraction was calculated and plotted after comparison with the corresponding controls (0 Gy). The sensitizing enhancement ratio (*SER*) was calculated as the ratio of the inactivation dose under scrambled siRNA control conditions divided by the inactivation dose after SAG silencing. Points, mean from three independent experiments; bars, SEM.

SAG silencing sensitizes H1299 and U87 cells to radiation. SAG was previously shown to have antioxidant activity and protected cells from redox compound–induced apoptosis (10, 12). Because a common mechanism by which radiation induced cell killing is through production of reactive oxygen species (25), we determined if SAG silencing would confer radiosensitivity to otherwise radioresistant cancer cells. Two radioresistant cell lines, H1299 and U87 (20, 26), were tested in a standard clonogenic assay. As shown in Fig. 3, SAG silencing significantly sensitized them to radiation with sensitizing enhancement ratios of 1.28 and 1.43, respectively (*top* and *middle*). To test whether normal cells are also sensitive to radiation on SAG silencing, we performed a comparable assay in MRC-5 cells. As shown in Fig. 3 (bottom), SAG silencing did not sensitize normal cells to radiation with a sensitizing enhancement ratio of 1.02. The findings suggest that SAG silencing selectively sensitizes cancer cells to radiation.

SAG silencing induces apoptosis with an accumulation of proapoptotic protein NOXA. To investigate the potential mechanism of cell growth suppression induced by SAG silencing, we performed FACS analysis to profile the cell population at the sub-G_1 (apoptotic population) or other phases of cell cycle in H1299 and U87 cells. As shown in Fig. 4A, 20% of the H1299 and U87 cell population underwent apoptosis on SAG silencing, compared with <5% of the population seen in LT-CONT control cells. The apoptotic induction of these cells on SAG silencing was further confirmed by the activation of caspase-3 (Fig. 4B). No significant cell cycle disturbance was induced by SAG silencing in both cell lines (data not shown). Furthermore, only a small fraction of SAG-silenced cells underwent senescence, as shown by senescence-associated β-gal staining, but without a significant difference from the control cells (data not shown). These results clearly show that apoptosis induced by SAG silencing is the major mechanism for the inhibition of cell growth and survival.

To further understand how SAG silencing induced apoptosis, we analyzed the expression of a panel of proapoptotic proteins (Bax, Bak, Puma, Bim, Bad, and NOXA), antiapoptotic proteins (Bcl-2, Mcl-1, survivin, XIAP, Bcl-XL, and cIAP2), and known SCF E3 ligase substrates (β-catenin, cyclin D, cyclin E, IκBα, p21, and pRB; refs. 4, 5). As shown in Fig. 4C, among the apoptosis regulatory

proteins tested, proapoptotic NOXA was the only protein significantly accumulated in both H1299 and U87 cells on SAG silencing. Other SCF E3 ligase substrates were either unchanged or undetectable, except pRB, which was accumulated in U87 cells as well as A549 cells, but not in H1299 cells (Supplementary Fig. S1). In addition, the expression of these proteins on SAG silencing was also determined in another lung cancer cell line, A549. Consistently, on SAG knockdown, NOXA was accumulated, whereas the other proteins were unchanged (Supplementary Fig. S1).

SAG overexpression reduces NOXA levels and shortens its protein half-life, whereas SAG knockdown extends NOXA half-life. As a RING component of SCF E3 ubiquitin ligases, SAG knockdown by siRNA would disrupt the

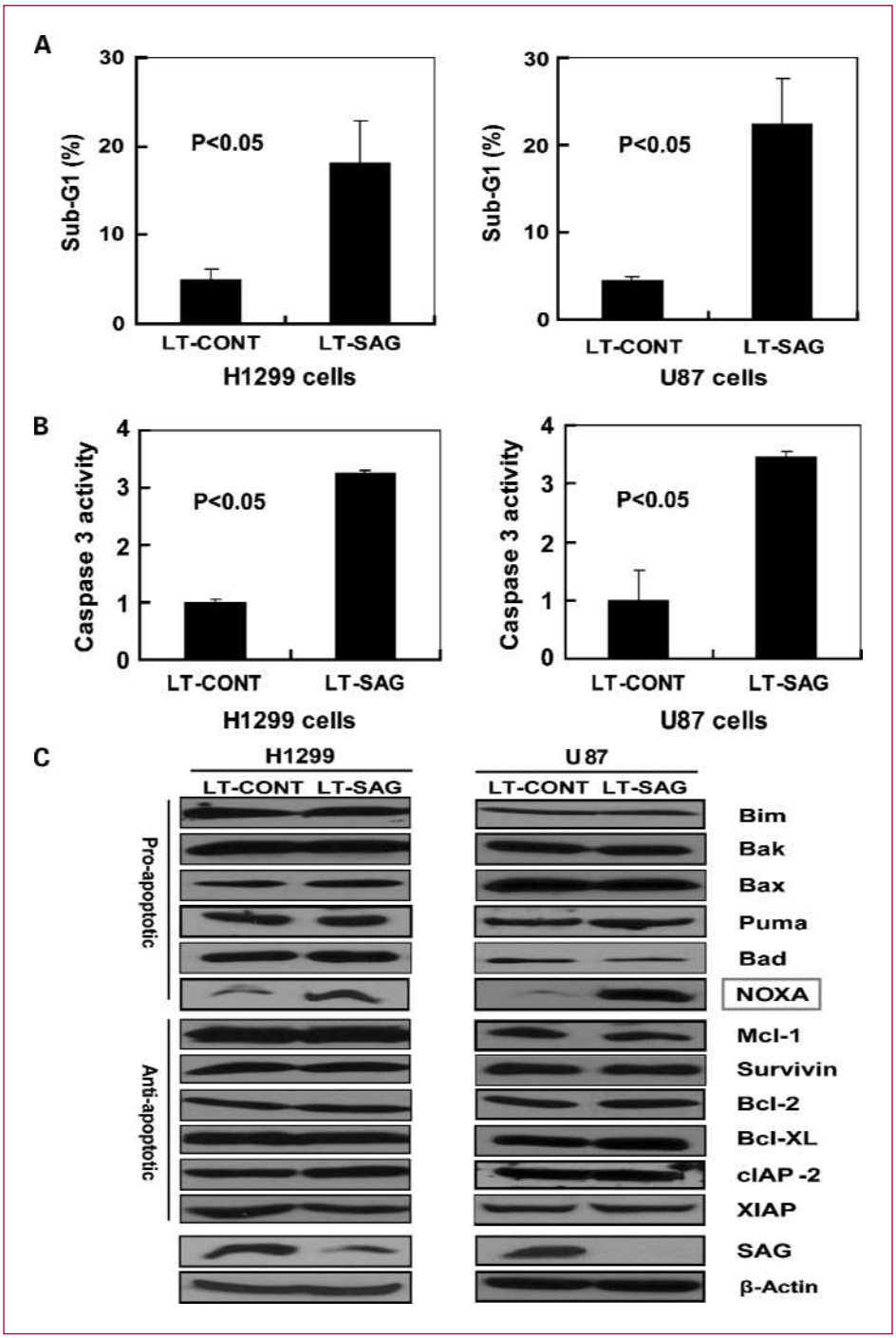

Fig. 4. SAG silencing induces apoptosis with NOXA accumulation. H1299 and U87 cells were infected with LT-SAG, along with LT-CONT, for 96 h, then split and cultured for 72 h, followed by propidium iodide staining and FACS analysis for apoptosis detection, caspase-3 activity assay, cell cycle profile, and Western blotting for the levels of apoptosis-associated proteins. A, induction of apoptosis by SAG silencing. Apoptotic cells were determined by sub-G_1 fraction in FACS analysis. B, caspase-3 activation on SAG silencing. Caspase-3 activity in infected cells was determined by caspase-3 activity assay. Columns, mean of three independent experiments; bars, SEM. C, expression of apoptosis-associated proteins. The status of a panel of apoptosis-associated proteins including proapoptosis proteins and antiapoptosis proteins were detected by Western blotting, with β-actin as the loading control.

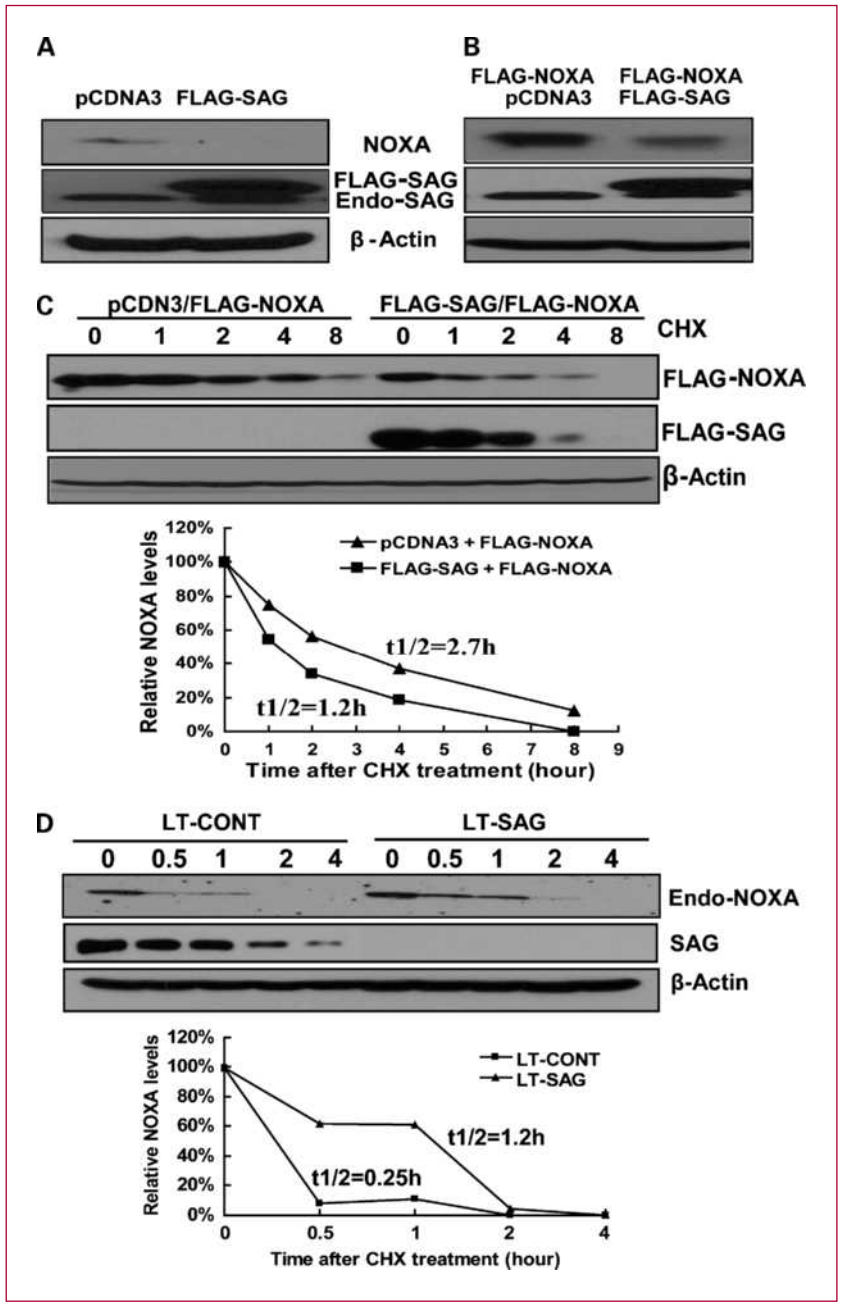

Fig. 5. SAG manipulation changes NOXA level and protein half-life. A, SAG overexpression eliminates endogenous NOXA. U87 cells were transiently transfected with pcDNA3-FLAG-SAG, along with pcDNA3 as a control. Cells were harvested 30 h later and subjected to Western blotting using anti-NOXA antibody, with β-actin as the loading control. B, SAG overexpression reduces the level of ectopically overexpressed NOXA. U87 cells were transiently cotransfected with FLAG-NOXA and FLAG-SAG or FLAG-NOXA and pcDNA3. Cells were harvested 30 h later and subjected to Western blotting using anti-FLAG antibody (for FLAG-NOXA) and anti-SAG (for FLAG-SAG and endogenous SAG), with β-actin as the loading control. C, SAG overexpression shortened the protein half-life of NOXA. U87 cells were transiently cotransfected with FLAG-NOXA and FLAG-SAG or FLAG-NOXA and pcDNA3. Twenty-four hours later, cells were treated with 20 μg/mL cycloheximide for the indicated periods of time, followed by Western blotting using antibodies against FLAG (for FLAG-NOXA) and SAG (for FLAG-SAG), with β-actin as the loading control. The relative NOXA levels were quantified by densitometry analysis using the ImageJ1.410 image processing software. D, SAG knockdown extended the half-life of endogenous NOXA. U87 cells were infected with LT-SAG, along with LT-CONT, for 96 h and then split. Twenty-four hours later, cells were treated with 20 μg/mL cycloheximide for the indicated periods of time, followed by Western blotting using antibody against endogenous NOXA, with β-actin as the loading control. The relative NOXA levels were quantified by densitometry analysis using the ImageJ1.410 image processing software. Endo-NOXA, endogenous NOXA.

SCF complex and inactivate its ligase activity, leading to the accumulation of its substrates, whereas SAG overexpression would likely promote the degradation of its substrates. We next characterized NOXA as a potential substrate of SAG SCF E3 ubiquitin ligases in U87 cells. Indeed, SAG overexpression eliminated endogenous NOXA (Fig. 5A), as well as reduced the level of ectopically overexpressed NOXA (Fig. 5B). Furthermore, SAG overexpression significantly shortened the protein half-life of NOXA from 2.7 to 1.2 hours (Fig. 5C). Finally, we evaluated the effects of SAG knockdown on the half-life of endogenous NOXA and found that SAG silencing significantly extended the half-life of NOXA from about 0.25 to 1.2 hours (Fig. 5D). Thus, NOXA seems to be a novel substrate of SAG E3 ligase.

SAG silencing inhibits the* in vivo *tumor growth in an orthotopic mouse model of pancreatic cancer. We next assessed the potential effect of SAG silencing on *in vivo* tumor growth using an orthotopic pancreatic tumor xenograft model because it is more physiologically relevant and far superior than subcutaneously implanted tumor models. We first confirmed that SAG expression

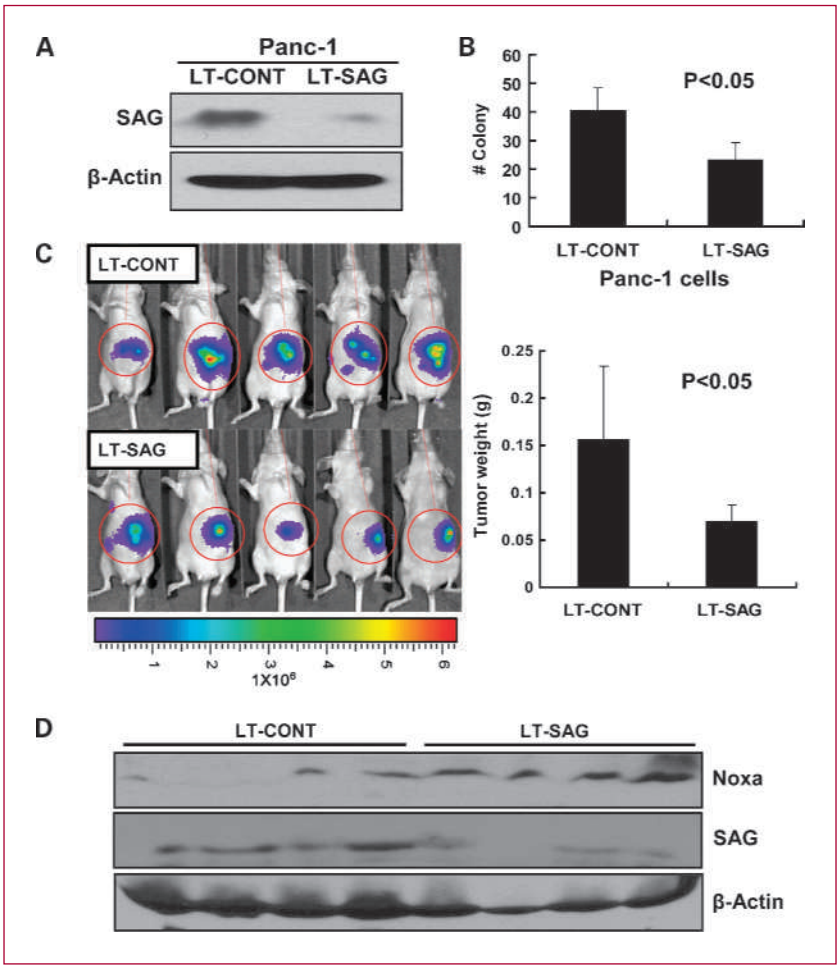

Fig. 6. SAG silencing inhibits the growth of orthotopic pancreatic tumors. PANC-1 human pancreatic carcinoma cells were infected with LT-CONT and LT-SAG, followed by determination of SAG silencing effect (A), cell survival assay *in vitro* (B), tumor formation *in vivo* (C), and Western blotting (D). A, SAG silencing effects. Panc-1 cells stably transfected with luciferase were infected with LT-CONT or LT-SAG, and SAG levels were determined 96 h postinfection by Western blotting, with β-actin as the loading control. B, clonogenic cell survival assay. Cells, after SAG silencing, were split, seeded into six-well plates at 100 per well in triplicates, and incubated at 37°C for 9 d, followed by 0.05% methylene blue staining and colony counting. C, bioluminescence imaging of implanted tumors and measurement of tumor weight. Panc-1 cells stably transfected with luciferase were infected with LT-CONT or LT-SAG and implanted into the pancreata of mice (five mice per group) for the evaluation of tumor growth *in vivo*. After 5 wks, tumors were bioluminescence imaged using a cryogenically cooled imaging system coupled to a data acquisition computer running Living Image software at the University of Michigan Small Animal Imaging Core. Mice were then sacrificed, and tumors were harvested and weighed. D, NOXA expression in tumors. The levels of Noxa and SAG in tumor tissues were determined by Western blotting using antibodies against NOXA and SAG, with β-actin as the loading control.

was indeed knocked down by LT-SAG in human pancreatic cancer PANC-1 cells by ~80% (Fig. 6A). Consistent to observations made in H1299 and U87 cells, SAG knockdown caused a 50% inhibition of PANC-1 cell survival *in vitro* (Fig. 6B). The SAG-silenced PANC-1 cells (LT-SAG), along with scrambled control cells (LT-CONT), were implanted into the pancreata of nude mice (five mice per group). After 5 weeks of *in vivo* growth, tumors were bioluminescence imaged. As shown in Fig. 6C (left), the strength of luminescent signal emitted from SAG-silenced tumors was, on average, much weaker than that from the control tumors. More precisely, each individual tumor was harvested and weighted. SAG silencing reduced overall tumor mass by 50%, which is statistically significant ($P < 0.05$; Fig. 6C, right). Finally, we determined the level of NOXA in available tumor tissues harvested and found that NOXA was accumulated in SAG-silenced tumors (Fig. 6D). Thus, the orthotopic *in vivo* growth of PANC-1 pancreatic cancer cells was significantly inhibited on SAG silencing, and NOXA accumulation may contribute to this process.

Discussion

Ideal cancer targets should have the following features: (*a*) they play an essential role in carcinogenesis, and/or are required for the maintenance of cancer cell phenotype, and/or are survival proteins that confer resistance to cancer cells against apoptosis; (*b*) they are overexpressed in cancer cells, which is associated with a poor prognosis of patient survival; (*c*) inhibition of their expression or activity induces growth suppression and/or apoptosis in cancer cells, but not in normal cells, achieving a potential therapeutic window; and (*d*) it is "druggable," that is, it is an enzyme (e.g., kinase) or a cell surface molecule (e.g., membrane-bound receptor) that can be easily screened for small-molecule inhibitors or being targeted by a specific antibody (27, 28). In this study, we validated SAG, a dual-function protein with antioxidant and ligase activities, as a potential anticancer target. We showed here that (*a*) SAG is overexpressed in several human cancers originated from different organs, particularly in lung cancer tissues; (*b*) SAG silencing, while having no effect on normal cell growth, dramatically inhibits proliferation and survival through apoptosis induction

in multiple cancer cell models in *in vitro* and in a pancreatic cancer orthotopic xenograft model *in vivo*; (*c*) SAG silencing also sensitizes radioresistant cancer cells to radiation. In combination with our previous studies that SAG, when overexpressed, protects cells from apoptosis induced by a variety of stimuli (10, 11, 15, 29) and promotes *in vivo* tumor growth also by inhibiting apoptosis (18) and the fact that SAG is a druggable E3 ubiquitin ligase, SAG seems to be a promising anticancer target as well as a target for radiosensitization.

Cancer cells tend to obtain apoptosis-escaping mechanisms by inactivating apoptosis signaling pathways through downregulation of proapoptotic proteins or upregulation of antiapoptotic proteins. Thus, reactivation of cellular apoptotic signaling has become a major effort toward the development of anticancer therapies (30, 31). In this study, we found that SAG silencing induced apoptosis, which was associated with the accumulation of proapoptotic NOXA. Further characterization revealed that SAG overexpression promoted the degradation of NOXA and shortened its protein half-life, whereas SAG knockdown delayed the degradation of NOXA and extended its half-life. Consistently, others have recently reported that NOXA was accumulated or upregulated after treatment with the proteasome inhibitor bortezomib (also known as Velcade, PS-341) in melanoma cells (32), and that NOXA, with a protein half-life of <2 hours in lymphoblastic leukemia cells, was subjected to ubiquitin-proteasome–mediated degradation, which is inhibited by a proteasome inhibitor, MG132 (33). Taken together, our study suggested that NOXA may be a novel substrate of SAG-SCF E3 ligase and its accumulation on SAG silencing could contribute to apoptosis induction. Future studies are directed to the identification of the F-box protein that recognizes NOXA for further biochemical characterization of NOXA as a novel substrate of SAG-SCF E3 ligase. Finally, given the fact that SAG is a RING component of SCF E3 ligases, required for ubiquitination and subsequent degradation of a variety of protein substrates, one could anticipate that alterations of multiple protein substrates would contribute to the induction of apoptosis following SAG silencing. Mechanistic characterization of more than 350 potential SCF E3 ligase substrates, identified through global protein stability profiling, which are closely involved in the regulation of apoptosis, cell cycle, and cell signaling (34, 35), would certainly broaden our understanding of how SAG-SCF E3 ligases regulate cell proliferation and apoptosis.

Radioresistance is a major obstacle for effective cancer treatment. Particularly in cases of glioblastoma multiforme and non–small cell lung cancer, radiotherapy is very ineffective due to the extreme radioresistance of cancer cells, contributing to poor patient survival rate (36, 37). Here, we showed that SAG silencing sensitized H1299 non–small cell lung cancer cells and U87 glioblastoma cells, two radioresistant lines, to radiation with the sensitizing enhancement ratio comparable with the silencing of TRAF2, a well-known cellular survival protein (20). Mechanistically, SAG silencing–mediated radiosensitization could be attributable to the loss of reactive oxygen species–scavenging activity that blocks radiation-generated reactive oxygen species (25). It has been previously shown that SAG overexpression protects cells or tissues against damages induced by the redox compound 1,10-phenanthroline or zinc ion (10, 13), nitric oxide (14), ischemia/hypoxia (15), neurotoxin and 1-methyl-4-phenylpyridinium (17), heat shock (16), and UV irradiation (38). On the other hand, radiosensitization on SAG silencing could result from the accumulation of a panel of yet-to-be-identified radiation-sensitizing substrates as a result of the inactivation of SAG SCF E3 ligase activity.

In summary, we validated SAG as a promising anticancer target as well as a target for radiosensitization on the basis of the following findings: (*a*) SAG is overexpressed in several human primary tumor tissues, particularly lung cancer; (*b*) SAG silencing selectively kills cancer cells, but not normal cells, *in vitro* and *in vivo*; and (*c*) SAG silencing sensitizes cancer cells to anticancer radiation. The future challenges will be (*a*) to identify specific inhibitors of SAG E3 ligases (27, 28) and to develop them as a novel class of anticancer agents and radiosensitizers, and (*b*) to develop siRNA-based therapy against radioresistant cancer using nanoparticle-packaged SAG siRNA (39, 40).

Disclosure of Potential Conflicts of Interest

No potential conflicts of interest were disclosed.

Acknowledgments

We thank Drs. Dafydd Thomas and Thomas Giordano for providing us the primary human cancer tissue microarrays.

Grant Support

National Cancer Institute grants CA111554 and CA118762 (Y. Sun).
The costs of publication of this article were defrayed in part by the payment of page charges. This article must therefore be hereby marked *advertisement* in accordance with 18 U.S.C. Section 1734 solely to indicate this fact.

Received 6/26/09; revised 10/22/09; accepted 11/19/09; published OnlineFirst 1/26/10.

References

1. Nalepa G, Rolfe M, Harper JW. Drug discovery in the ubiquitin-proteasome system. Nat Rev Drug Discov 2006;5:596–613.
2. Orlowski RZ. Proteasome inhibitors in cancer therapy. Methods Mol Biol 2005;301:339–50.
3. Nikiforov MA, Riblett M, Tang WH, et al. Tumor cell-selective regulation of NOXA by c-MYC in response to proteasome inhibition. Proc Natl Acad Sci U S A 2007;104:19488–93.
4. Nakayama KI, Nakayama K. Ubiquitin ligases: cell-cycle control and cancer. Nat Rev Cancer 2006;6:369–81.
5. Petroski MD, Deshaies RJ. Function and regulation of cullin-RING ubiquitin ligases. Nat Rev Mol Cell Biol 2005;6:9–20.

6. Frescas D, Pagano M. Deregulated proteolysis by the F-box proteins SKP2 and β-TrCP: tipping the scales of cancer. Nat Rev Cancer 2008;8:438–49.
7. Welcker M, Clurman BE. FBW7 ubiquitin ligase: a tumour suppressor at the crossroads of cell division, growth and differentiation. Nat Rev Cancer 2008;8:83–93.
8. Mao JH, Kim IJ, Wu D, et al. FBXW7 targets mTOR for degradation and cooperates with PTEN in tumor suppression. Science 2008;321: 1499–502.
9. Jia L, Soengas MS, Sun Y. ROC1/RBX1 E3 ubiquitin ligase silencing suppresses tumor cell growth via sequential induction of G_2-M arrest, apoptosis, and senescence. Cancer Res 2009;69:4974–82.
10. Duan H, Wang Y, Aviram M, et al. SAG, a novel zinc RING finger protein that protects cells from apoptosis induced by redox agents. Mol Cell Biol 1999;19:3145–55.
11. Sun Y, Tan M, Duan H, Swaroop M. SAG/ROC/Rbx/Hrt, a zinc RING finger gene family: molecular cloning, biochemical properties, and biological functions. Antioxid Redox Signal 2001;3:635–50.
12. Swaroop M, Bian J, Aviram M, et al. Expression, purification, and biochemical characterization of SAG, a RING finger redox sensitive protein. Free Radic Biol Med 1999;27:193–202.
13. Sun Y. Alteration of SAG mRNA in human cancer cell lines: requirement for the RING finger domain for apoptosis protection. Carcinogenesis 1999;20:1899–903.
14. Yang ES, Park JW. Regulation of nitric oxide-induced apoptosis by sensitive to apoptosis gene protein. Free Radic Res 2006;40:279–84.
15. Chanalaris A, Sun Y, Latchman DS, Stephanou A. SAG attenuates apoptotic cell death caused by simulated ischaemia/reoxygenation in rat cardiomyocytes. J Mol Cell Cardiol 2003;35:257–64.
16. Lee SJ, Yang ES, Kim SY, Shin SW, Park JW. Regulation of heat shock-induced apoptosis by sensitive to apoptosis gene protein. Free Radic Biol Med 2008;45:167–76.
17. Kim SY, Kim MY, Mo JS, Park JW, Park HS. SAG protects human neuroblastoma SH-SY5Y cells against 1-methyl-4-phenylpyridinium ion (MPP+)-induced cytotoxicity via the downregulation of ROS generation and JNK signaling. Neurosci Lett 2007;413:132–6.
18. Gu Q, Bowden TG, Normolle D, Sun Y. SAG/ROC2 E3 ligase regulates skin carcinogenesis by stage dependent targeting of c-Jun/AP1 and IκB/NF-κB. J Cell Biol 2007;178:1009–23.
19. Sasaki H, Yukiue H, Kobayashi Y, et al. Expression of the sensitive to apoptosis gene, SAG, as a prognostic marker in nonsmall cell lung cancer. Int J Cancer 2001;95:375–7.
20. Zheng M, Morgan-Lappe SE, Yang J, et al. Growth inhibition and radiosensitization of glioblastoma and lung cancer cells by small interfering RNA silencing of tumor necrosis factor receptor-associated factor 2. Cancer Res 2008;68:7570–8.
21. Gu Q, Tan M, Sun Y. SAG/ROC2/Rbx2 is a novel activator protein-1 target that promotes c-Jun degradation and inhibits 12-*O*-tetradecanoylphorbol-13-acetate-induced neoplastic transformation. Cancer Res 2007;67:3616–25.
22. Bockbrader KM, Tan M, Sun Y. A small molecule Smac-mimic compound induces apoptosis and sensitizes TRAIL-and etoposide-induced apoptosis in breast cancer cells. Oncogene 2005;24: 7381–8.
23. Khanbolooki S, Nawrocki ST, Arumugam T, et al. Nuclear factor-κB maintains TRAIL resistance in human pancreatic cancer cells. Mol Cancer Ther 2006;5:2251–60.
24. Huang Y, Duan H, Sun Y. Elevated expression of SAG/ROC2/Rbx2/Hrt2 in human colon carcinomas: SAG does not induce neoplastic transformation, but its antisense transfection inhibits tumor cell growth. Mol Carcinog 2001;30:62–70.
25. Cook JA, Gius D, Wink DA, Krishna MC, Russo A, Mitchell JB. Oxidative stress, redox, and the tumor microenvironment. Semin Radiat Oncol 2004;14:259–66.
26. Wang CC, Liao YP, Mischel PS, Iwamoto KS, Cacalano NA, McBride WH. HDJ-2 as a target for radiosensitization of glioblastoma multiforme cells by the farnesyltransferase inhibitor R115777 and the role of the p53/p21 pathway. Cancer Res 2006;66:6756–62.
27. Sun Y. Targeting E3 ubiquitin ligases for cancer therapy. Cancer Biol Ther 2003;2:623–9.
28. Sun Y. E3 ubiquitin ligases as cancer targets and biomarkers. Neoplasia 2006;8:645–54.
29. Yang GY, Pang L, Ge HL, et al. Attenuation of ischemia-induced mouse brain injury by SAG, a redox-inducible antioxidant protein. J Cereb Blood Flow Metab 2001;21:722–33.
30. Fulda S. Inhibitor of apoptosis proteins as targets for anticancer therapy. Expert Rev Anticancer Ther 2007;7:1255–64.
31. Nicholson DW. From bench to clinic with apoptosis-based therapeutic agents. Nature 2000;407:810–6.
32. Fernandez Y, Verhaegen M, Miller TP, et al. Differential regulation of noxa in normal melanocytes and melanoma cells by proteasome inhibition: therapeutic implications. Cancer Res 2005;65:6294–304.
33. Ploner C, Rainer J, Lobenwein S, Geley S, Kofler R. Repression of the BH3-only molecule PMAIP1/Noxa impairs glucocorticoid sensitivity of acute lymphoblastic leukemia cells. Apoptosis 2009;14:821–8.
34. Yen HC, Elledge SJ. Identification of SCF ubiquitin ligase substrates by global protein stability profiling. Science 2008;322:923–9.
35. Yen HC, Xu Q, Chou DM, Zhao Z, Elledge SJ. Global protein stability profiling in mammalian cells. Science 2008;322:918–23.
36. Short SC. External beam and conformal radiotherapy in the management of gliomas. Acta Neurochir Suppl 2003;88:37–43.
37. Spiro SG, Silvestri GA. One hundred years of lung cancer. Am J Respir Crit Care Med 2005;172:523–9.
38. He H, Gu Q, Zheng M, Normolle D, Sun Y. SAG/ROC2/RBX2 E3 ligase promotes UVB-induced skin hyperplasia, but not skin tumors, by simultaneously targeting c-Jun/AP-1 and p27. Carcinogenesis 2008;29:858–65.
39. de Fougerolles AR. Delivery vehicles for small interfering RNA *in vivo*. Hum Gene Ther 2008;19:125–32.
40. Howard KA, Kjems J. Polycation-based nanoparticle delivery for improved RNA interference therapeutics. Expert Opin Biol Ther 2007;7: 1811–22.